Title

Carbidopa Effect on ^{18}F-FDOPA Uptake in Insulinoma: from Cell Culture to microPET Imaging

Short Title

Preclinical ^{18}F-FDOPA PET in Insulinoma

Authors and affiliations

Julien Detour[1,2], Alice Pierre[1,2], Fréderic Boisson[3], Guillaume Kreutter[4,5], Thomas Lavaux[6], Izzie Jacques Namer[2,5,7], Laurence Kessler[4,5,8], David Brasse[3], Patrice Marchand[3] and Alessio Imperiale[2,3,5,7]

(1) Radiopharmacy, Strasbourg University Hospitals, Strasbourg, France

(2) Biophysics and Nuclear Medicine, Strasbourg University Hospitals, Strasbourg, France

(3) Institut Pluridisciplinaire Hubert Curien (IPHC), CNRS/UMR7178, Strasbourg University, Strasbourg, France

(4) EA7293, Vascular and Tissular Stress in Transplantation, Illkirch, France

(5) Federation of Translational Medicine of Strasbourg (FMTS), Faculty of Medicine, Strasbourg University, Strasbourg, France

(6) Biochemistry and Molecular Biology, Strasbourg University Hospitals, Strasbourg, France

(7) ICube, CNRS/UMR 7357, Strasbourg University, Strasbourg, France

(8) Diabetology, Strasbourg University Hospitals, Strasbourg, France.

First Author:

Julien Detour, PharmD, PhD

Radiopharmacy / Biophysics and Nuclear Medicine

Hautepierre University Hospital

1, Avenue Molière, 67098 Strasbourg Cedex, France

Tel : +33388127825

Fax : +33388128121

Email: julien.detour@chru-strasbourg.fr

Corresponding Author:

Alessio Imperiale, MD, PhD

Biophysics and Nuclear Medicine

Hautepierre University Hospital

1, Avenue Molière, 67098 Strasbourg Cedex, France

Tel : +33388127552

Fax : +33388128121

Email: alessio.imperiale@chru-strasbourg.fr

Word count: Abstract: 212, Document: 5088, **Tables:** 0, **Figures:** 5

Disclosure summary: The authors have nothing to disclose.

ABSTRACT

Patient premedication by carbidopa seems to improve the accuracy of 6-^{18}F-fluoro-3,4-dihydroxy-L-phenylalanine (^{18}F-FDOPA) positron emission tomography (PET) for insulinoma diagnosis. However, the risk of PET false negative result has been evoked using carbidopa. Consequently, we aim to evaluate the effect of carbidopa on ^{18}F-FDOPA uptake in insulinoma beta cells and insulinoma xenograft model in mice. **Methods:** ^{18}F-FDOPA *in vitro* accumulation was assessed in the murine beta cell line RIN-m5F. The *in vivo* microPET experiments were performed on tumor-bearing nude mice after subcutaneous injection of RIN-m5F cells. Experiments were conducted with and without carbidopa pretreatment. **Results:** Incubation of RIN-m5F cells with 80 µM of carbidopa did not significantly affect the cellular accumulation of ^{18}F-FDOPA. Tumor xenograft was clearly detectable by microPET in all cases. Carbidopa-treated mice showed significantly higher ^{18}F-FDOPA uptake on the insulinoma xenografts than non-treated mice. Irrespectively of carbidopa premedication, the xenograft was characterized by an early increase of ^{18}F-FDOPA uptake followed by a progressive reduction over time. **Conclusions:** Carbidopa does not influence the *in vitro* ^{18}F-FDOPA uptake accumulation in RIN-m5f cells but improves insulinoma imaging *in vivo*. Our findings increase the current knowledge about ^{18}F-FDOPA uptake profile of RIN-m5F cells and related xenograft model. The present work represents the first preclinical research specifically focused on the insulinoma with potential translational implication.

Keywords: ^{18}F-FDOPA, PET, insulinoma, carbidopa, small animal PET, RIN-m5F

Insulinoma is a rare, usually solitary and benign neuroendocrine tumor (NET). Insulinoma is characterized by inappropriate and uncontrolled insulin production and secretion with consequent glycopenic symptoms and potentially lethal hypoglycemia. Early detection of the tumor is crucial, allowing curative treatment by surgical enucleation. Nowadays, localization of insulinoma remains challenging and the conventional imaging is the first line diagnostic investigation (1).

Functional imaging may be of particular interest when conventional imaging is negative or inconclusive (2). Nevertheless, the gold-standard examination remains to be defined. Radiolabelled glucagon like peptide-1 analogues used for conventional scintigraphic studies or PET imaging have shown promising results since glucagon like peptide-1 receptors are overexpressed in most insulinomas (3). However, these radiopharmaceuticals are not yet commercially available and are used in humans mostly in clinical trials. ^{18}F-FDOPA is clinically approved and commercially available in many countries for PET imaging of insulinoma. Once internalized by specific cell-membrane transporters, ^{18}F-FDOPA is decarboxylated in ^{18}F-dopamine by the aromatic amino acid decarboxylase (AADC), and accumulated into secretory vesicles. Therefore, the expression of AADC has a key role in tumor visualization by ^{18}F-FDOPA PET (4). However, the intense and prolonged radiotracer uptake by the mature exocrine pancreas represents the main drawback of ^{18}F-FDOPA PET that may explain the initial disappointing results for insulinoma detection (5). Furthermore, early PET images and patient premedication by carbidopa may improve the diagnostic accuracy of ^{18}F-FDOPA PET in adult patients with insulinoma-related hyperinsulinemic hypoglycemia (6,7). Carbidopa is an efficient inhibitor of the AADC capable of drastically reducing the physiological pancreatic uptake with consequent increase of the tumor to background ratio (8). Moreover, carbidopa leads to better systemic

radiotracer availability by reducing the peripheral conversion of ^{18}F-FDOPA to ^{18}F-dopamine and its renal excretion. However, no final consensus has been reached about the usefulness of carbidopa premedication before ^{18}F-FDOPA PET in patients with hyperinsulinemic hypoglycemia because of potential reduction of tumoral uptake intensity (9). The risk of ^{18}F-FDOPA PET false negative results could be high for tumors with low intracellular AADC activity (10), which are potentially more sensitive to the inhibitory effect of carbidopa.

The positive impact of carbidopa premedication has been demonstrated in both *in vitro* and *in vivo* studies using cell lines of human pancreatic NET (BON cells) and related tumor xenograft animal model (11,12). To the best of our knowledge, no preclinical data are available concerning the influence of carbidopa on ^{18}F-FDOPA uptake in insulinoma. Therefore, we aim to evaluate the effect of carbidopa on ^{18}F-FDOPA uptake in the beta cell line RIN-m5F and the related insulinoma xenograft model developed in nude mice. The present work represents the first preclinical research study focused on insulinoma, with potential impact on the diagnostic and therapeutic management of patients in clinical practices.

MATERIALS AND METHODS

Radiotracer Production

GMP-compliant ^{18}F-FDOPA was obtained from CISBIO International (DOPACIS, Nancy, France) and was synthesized by electrophilic substitution following the method reported by de Vries et al. (13). A total activity of 200-240 MBq in 2.2 mL was received and further diluted with 0.9 % sterile NaCl to reach an injection volume of 150 μL.

Cell Culture

In vitro experiments were performed with the beta cell line RIN-m5F (ATCC CRL-11605[TM]) (*14*). These cells produce and secrete insulin, and produce AADC. Unlike the parental line they do not produce somatostatin. Positive ^{18}F-FDOPA uptake in cell line RIN-m5F has been previously reported (*15*). Cells were cultured in 75 cm² culture flasks containing 20 mL of Roswell Park Memorial Institute medium (RPMI 1640) without N-2-hydroxyethylpiperazine-N-2-ethane sulfonic acid, and glutamine (Invitrogen, UK). Medium was supplemented with 10% foetal bovine serum (Gibco, USA) and 100 µg/mL of Gentamycine (Panpharma, France). Cells were grown at 37°C in a humified atmosphere containing 5% CO_2 and subcultured twice a week.

In Vitro Determination of ^{18}F-FDOPA Accumulation

Flasks were maintained at 37°C and incubated 1h either with or without 80 µM of carbidopa (INRESA, France). In another condition, 2 hours before experiment, RPMI culture medium was replaced by an amino acid free medium composed of phosphate buffer PBS (0.9 mM $CaCl_2$, 0.5 mM $MgCl_2$, 2.6 mM KCl, 1.47 mM KH_2PO_4, 138 mM NaCl, 8 mM Na_2HPO_4, pH=7; Gibco, New York, USA) and glucose (D-glucose 0.75 mM). Then 200 kBq of buffered ^{18}F-FDOPA were added to each flask within the culture medium (dissolved in a volume of 100 µL to 150µL). After 5, 30 and 60 minutes the culture medium or PBS-Glu buffer was removed; cells were washed, harvested by trypsin treatment, and suspended in the same type and volume of culture medium (RPMI or PBS-Glu). A volume of 2.5 mL of culture cells or of removed medium was transferred in 5 mL counting tubes and radioactivity was measured in a calibrated gamma counter (Wallac, Perkin Elmer, USA). For non-specific tracer adsorption the protocol was

reproduced identically without cells. The viability and number of cells were determined with the trypan blue exclusion technique using a Kova Glastic Slide 10 (Hycor Biomedical, Kassel, Germany).

In a similar experiment methodology using RPMI as culture medium, cells were also incubated separately with 10 mM of 2-aminobicyclo[2.2.1]heptane-2-carboxylic acid (BCH), described as a L-amino acid-transporter inhibitor (*16*) and 10 µM of Tetrabenazine described as an inhibitor of the vesicular monoamine transporter (*17*).

Animals

Twenty female athymic nude mice (24–28 g, 8–10 weeks-old, Charles Rivers) were used in the entire experimental protocol. In order to optimize the management of the insulinoma xenograft mice, the carbidopa administration and the PET imaging protocol, ten out of twenty animals (control group) were used to assess the morphological evolution of the tumor xenograft (i.e.: tumor size) and the related consequences of tumor insulin secretion on the animal welfare (i.e.: reduction of serum glycemia and lethal hypoglycemia occurrence). The remaining ten mice (experimental group) were dedicated to *in vivo* microPET investigations of insulinoma xenograft. Animals were kept at constant temperature (22 °C) and humidity (40%) with 12h light/dark cycles and were allowed free access to forage and water until the beginning of each imaging procedure. Animals were housed in individually ventilated cages with HEPA filters in the dedicated facility of the Hubert Curien Institut (IPHC) at Strasbourg.

Tumor Xenograft Mice

A cell suspension of six million RIN-m5F cells in 100 μL of PBS was injected subcutaneously in the mice right hind leg under inhalation anesthesia (1.5-2% of isoflurane). Tumor width and length were measured (mm) with a caliper to calculate the tumor volume according to the approximated formula: Volume=(length)x(width^2)/2 (mm^3). To evaluate the insulin production, morning serum glycemia levels in the xenograft mice were assessed from blood samples collected from the tail vein of non-fasted mice by a commercial blood glucose monitoring system (Contour TS, Bayer).

^{18}F-FDOPA microPET Imaging

Animals were scanned when the tumor reached the minimum dimension of 2.5x2.5 mm^2 or a volume of greater than 20 mm^3. Mice were divided into two groups according to carbidopa pretreatment (i.e.: carbidopa-treated or non-treated mice). Carbidopa was administered *per os* via a gavage needle at the dose of 20 μg in 100 μL of NaCl one hour prior to the intravenous (i.v.) injection of ^{18}F-FDOPA. In all animals, ^{18}F-FDOPA was injected through the jugular vein and PET images were acquired on a small-animal PET scanner (Iris, Inviscan) with a spatial resolution below 1.4 mm in the reconstructed PET images. As a preventive measure, 300 μL of 20% glucose solution were administrated orally using a gavage needle thirty minutes before imaging procedure. For microPET imaging, ketamine and xylazine anesthesia was induced by an intraperitoneal injection of 50 mg/kg ketamine, 6 mg/kg xylazine in a volume of 100 μL/30 g body weight, and maintained with 1.5% isoflurane in medical air during the entire procedure using a calibrated vaporizer. Twenty minutes dynamic 3D PET acquisitions were performed

starting 2 min after the ^{18}F-FDOPA injection. During PET acquisition, animal temperature and respiration rate were monitored to assess the depth of anesthesia. Throughout the whole investigation, mice were held at a constant temperature of 37° C.

Acquired list-mode PET data were binned into four frames of 5-min each and twenty frames of 1-min each. Data were reconstructed into a 201x201x120 3D volume using the iterative 3D-OSEM algorithm with 6 iterations and 8 subsets. The voxel size is equal to 0.42 mm in the transverse plane and 0.85 mm in the axial direction. The calibration factor was included in the normalization file and applied during reconstruction process. PET data were fully corrected for random coincidences, radioactive decay and dead-time. No attenuation and scatter corrections were applied.

^{18}F-FDOPA PET images analysis was performed using the AMIDE software package (http://amide. sourceforge.net/). microPET images were qualitatively interpreted as positive or negative. A focal non-physiologic increase in radiotracer uptake in the area of tumor development was considered as positive PET result. For a semi-quantitative assessment of tumoral ^{18}F-FDOPA uptake, an elliptical volume of interest (VOI) was drawn on the tumor using the image resultant from the first 5 min PET acquisition. Tumoral VOI activity was first corrected by the mean voxel value measured in the contralateral thigh muscle. Afterwards, only voxels higher than 40% of the maximum voxel value in the tumor were considered for further analysis. Elliptical VOIs were also drawn on the pancreas, liver, and mediastinum. Finally, time-activity curves were extracted from VOIs over the whole dynamic PET acquisition. Standardized Uptake Values (SUVs) were calculated using the mean voxel value within the VOIs. SUVs were recorded and used for generating time-activity curves.

All animal experiments were performed in accordance with the European Institutes of Health Guidelines regarding the care and use of animals for experimental procedures and were approved by the Alsace Regional Ethics Committee for Animal Experimentation (Approval ID: APAFIS#2944).

Data Analysis

Differences between various groups were tested for statistical significance using non-parametric test such as Friedmann test for repeated measures with adapted post hoc tests and Mann-Whitney U-test for independent samples as appropriate. The justification of such statistic is based on a low number of samples in some condition. For convenient purpose results are represented as mean ± standard error of mean. *p<0.05* was considered as significant. Statistical analysis was performed using SPSS Statistics (IBM) software package.

RESULTS

In Vitro Determination of ^{18}F-FDOPA Accumulation

Control Condition. The accumulation of ^{18}F-FDOPA in cells incubated in RPMI culture medium was almost constant over 60 min. Only a slight increase of ^{18}F-FDOPA uptake was observed ranging from $2.9\%/10^6$ cells at 5 min to $4.5\%/10^6$ cells at 60 min. In the control condition with amino acid-free PBS-Glu medium the cellular ^{18}F-FDOPA uptake decreases over time of about 3.7% ranging from $6.8\%/10^6$ cells at 5 min to $3.1\%/10^6$ cells at 60 min (Fig. 1A). The highest amount of radiotracer uptake was observed at the earliest time point (5 min) and was

more than twice higher as compared to the RPMI medium condition. No statistically significant differences were observed within each culture condition over the three tested time points neither with the standard culture medium nor with the amino acid-free PBS-Glu buffer medium (p=0.395 and p=0.135, respectively). Nonetheless statistical significance was observed in the control condition between the two culture media at the first (p<0.01) and last time points (p<0.05).

Inhibition Experiments. Incubation of cells with 80 µM of carbidopa did not significantly affect ^{18}F-FDOPA accumulations in RIN-m5F cells. Likely to the control condition, two different dynamic ^{18}F-FDOPA uptake patterns were observed according to the culture medium. In standard condition (RPMI culture medium), cells showed a quite stable ^{18}F-FDOPA uptake over time. In PBS-Glu medium, the ^{18}F-FDOPA uptake was highest at the earliest time point (5 min) and decreased over time ranging from 4.6%/10^6 cells at 5 min to 3.3%/10^6 cells at 60 min (Fig. 1A). Overall, no statistically significant differences of ^{18}F-FDOPA uptake were observed between carbidopa-treated and non-treated cells at the three-tested time points of incubation neither with the RPMI culture medium nor with the PBS-Glu buffer medium. BCH, a selective inhibitor of the L-amino acid-transporter, drastically lowered the tracer uptake at all studied time points in a statistically significant manner (p<0.05). Tetrabenazine led to a similar constant decrease of ^{18}F-FDOPA uptake over the studied period (p<0.05) (Fig. 1B).

Tumor Xenograft Mice and ^{18}F-FDOPA microPET Imaging

Control Group. Subcutaneous tumor xenograft was visible about 2 weeks after cellular inoculation of RIN-m5F cell suspension reaching a volume of at least 20 mm^3 about 3 weeks after cellular injection. Serial measurements of morning serum glycemia levels performed before and after the subcutaneous cellular injection highlighted a progressive decrease of blood glucose

concentration in mice, confirming the secreting character of the insulinoma xenograft (Fig. 2A). Consequently, water was replaced by a 20% glucose solution 15 days after the subcutaneous injection of RIN5-mF cells suspension in attempt to limit the severity of glycopenic symptoms (decrease of spontaneous activity followed by no activity, tremor, tachypnea or hypopnea) and to reduce the occurrence of lethal hypoglycemia in animals. No significant correlation was observed between the glycemia value and the insulinoma xenograft size. Pathological examination of tumor xenograft was performed in two mice, which died after a hypoglycemic crisis (Fig. 2B). Analysis revealed the presence of epithelioid and spindle cells staining for insulin (Figs. 2C and 2D).

Experimental Group. Despite the use of a 20% glucose solution instead of water, four animals died of hypoglycemic crisis within 12 days after inoculation of RIN-m5F cells suspension and before the appearance of measurable insulinoma xenograft. Hence, six mice underwent ^{18}F-FDOPA microPET investigations. Two experimental groups were considered consisting in 3 mice each. Animals from the first group were pretreated with 20 µg of carbidopa about one hour prior to the intravenous (i.v.) injection of ^{18}F-FDOPA (5.1±0.9 MBq in 150 µl). Mice from the second group received no premedication before ^{18}F-FDOPA i.v. administration (7.5±1.2 MBq in 150 µl). MicroPET studies were performed 3-4 weeks after the inoculation of RIN-m5F cells suspension and the tumor xenograft volume ranged from 20 to 159 mm^3. No significant difference of tumor size was observed between carbidopa-treated (77±42 mm^3) and non-treated mice (53±22 mm^3) and glycemia was lower than 60 mg/dL in all cases. Glycemia values and insulinoma size were not significantly correlated.

The tumor xenograft was clearly detectable in all mice irrespectively of carbidopa premedication (Fig. 3). The mean time-activity curves resulting from the tumor xenograft of both

carbidopa-treated and non-treated mice are reported in Figure 4. The dynamic profile of tumoral ^{18}F-FDOPA uptake was similar between carbidopa-treated and non-treated mice. The insulinoma xenograft was characterized by an early increase of ^{18}F-FDOPA uptake after radiotracer injection reaching the peak intensity about 5 minutes after the radiotracer injection. Then, the ^{18}F-FDOPA uptake progressively decreased over time until the end of the dynamic PET acquisition (about 35% reduction of initial SUV value). Tumor remained well detectable during the whole PET examination in carbidopa-treated and non-treated animals (Fig. 3).

There was no negative influence of carbidopa on tumoral ^{18}F-FDOPA uptake in animals pretreated with carbidopa. On the contrary, insulinoma xenografts from carbidopa-treated mice showed significantly higher ^{18}F-FDOPA uptake ($p<0.05$) over the whole PET acquisition than tumors developed in non-treated mice (Fig. 4).

Visually, carbidopa-treated mice showed increased ^{18}F-FDOPA uptake in abdominal organs such as pancreas and liver (Fig. 5), which could be explained by reduced peripheral radiotracer degradation by carbidopa and consequent increased availability for both tumor and abdominal organs. The statistical significance was not reached probably because of the small number of analyzed animals.

DISCUSSION

To the best of our knowledge, this is the first study that evaluates the effect of carbidopa on ^{18}F-FDOPA uptake in beta cells and the related xenograft model in mice. The most important conclusions include: (1) carbidopa does not induce significant differences in ^{18}F-FDOPA uptake intensity in the beta cell line RIN-5mF; (2) no negative influence was observed on PET detection of insulinoma xenograft in mice premedicated by carbidopa. On the contrary, carbidopa treatment significantly improves ^{18}F-FDOPA uptake in the RIN-m5F tumor xenograft.

The accumulation of ^{18}F-FDOPA in RIN-5mF cells was sensitive to the presence of amino acids within the culture medium. In RPMI medium, ^{18}F-FDOPA cellular uptake was almost constant over 60 min. On the other hand, an important increase of ^{18}F-FDOPA uptake at the earliest time point (5 min), followed by a progressive reduction was observed in amino acid-free medium. An early competition for cellular intake between ^{18}F-FDOPA and other amino acids present in the RPMI medium could support this observation.

No statistically significant effect was observed on RIN-5mF cells, concerning the uptake of ^{18}F-FDOPA over time regardless of the culture medium. This finding indicates that intracellular decarboxylation process in RIN-5mF cells was not considerably affected by the pharmacological inhibition of carbidopa. The up-regulation of AADC activity in NET cells supports these results (*10,17*).

To our knowledge no previous experimental data discussing the effect of carbidopa on RIN-5mF cell line have been reported to allow further comparison. However, similar investigations have been previously performed on BON NET cells. According to Neels et al. (*11*), the incubation of BON cells with carbidopa did not affect the accumulation of ^{18}F-FDOPA, neither in full culture medium nor in PBS-Glu buffer media. Moreover, the accumulation of ^{18}F-FDOPA was more rapid and much higher in amino acid–free PBS-Glu buffer than in standard culture medium. These results were partially confirmed by Kuik et al. (*12*), who recently reported significant decrease in ^{18}F-FDOPA accumulation after carbidopa treatment only at late time points under amino acids depletion condition.

The experiment performed under BCH inhibition underlines the importance of amino acids metabolic pathway in RIN-5mF cells. The deregulation of amino acid intake by specific

pharmacological agents targeting L-amino acid-transporter may emerge as an interesting therapeutic option as previously observed during *in vitro* and *in vivo* studies in gliomas (*18*).

Tetrabenazine led to a similar but lesser extent decrease of ^{18}F-FDOPA uptake than those observed with BCH. In this experimental condition, ^{18}F-dopamine is not transported into the cellular granules by vesicular monoamine transporters and thus potentially cleared from the cell.

The advantage of carbidopa administration has been suggested in mice with NET xenograft from BON cells and in patients with pancreatic NET (*11,19*). Carbidopa improved image interpretation for ^{18}F-FDOPA PET by increasing tumoral uptake and lowering the physiological pancreatic accumulation. We observed similar effect in nude mice bearing a RIN-m5F insulinoma xenograft. Accordingly, under carbidopa inhibition, the ^{18}F-FDOPA uptake was significantly higher than in non-treated mice.

In our study, the carbidopa administration protocol was optimized before PET imaging. The combination of repeated anesthesia and the physical trauma due to intraperitoneal injections of carbidopa was poorly tolerated in weakened mice with insulinoma-related chronic hypoglycemia. For this reason, in the experimental group, the carbidopa was administrated orally 1 hour before the microPET imaging.

Overall, the absence of tumoral inhibition, the low physiological pancreatic uptake, and the increase of ^{18}F-FDOPA availability could be considered as the underlying effects of carbidopa premedication even in RIN-m5F insulinoma xenograft model.

Irrespective of carbidopa premedication, RIN-m5f insulinoma xenograft showed the highest uptake of ^{18}F-FDOPA within 5 min after radiotracer injection, followed by continuous decrease until the end of the studied period. This kinetic pattern is close to that observed *in vitro* using a culture media supplemented in D-glucose (PBS-Glu buffer medium). The oral overload of

glucose before microPET imaging may contribute to explain the results of *in vivo* experiments.

We have recently reported insulinomas showing a pathological ^{18}F-FDOPA uptake exclusively on early images in patients who underwent carbidopa-assisted PET/CT (*6,7*). In these cases, the influence of carbidopa on rapid tumoral wash-out can not completely be ruled out. In our preclinical model, the dynamic profile of ^{18}F-FDOPA uptake was similar in both carbidopa-treated and non-treated mice. Hence, the carbidopa premedication seems not directly related to the dynamic pattern of ^{18}F-FDOPA uptake. Kauhanen et al. (*9*) reported the disappearance of ^{18}F-FDOPA focal pancreatic uptake after carbidopa administration in two patients with histologically proven insulinoma and beta-cell hyperplasia. In these cases, the negative PET result could be more likely related to the non-optimized PET acquisition protocol rather than carbidopa-related tumoral inhibition. Beside, parallel ^{18}F-FDOPA catabolic pathways through for example catechol-O-methyl transferase deserves further investigation.

Significant differences between mice and humans should be taken into consideration in terms of methodological issue regarding carbidopa dose, inter species carbidopa metabolization, fasted conditions and glucose charge before PET. Moreover, the growing pattern of our tumor xenograft was more rapid than that of human insulinomas that are typically benign. Thus, caution in interpreting preclinical data is required. The malignant potential of our xenograft may have been amplified by the athymic status of the host (nude mice) and by the several cellular subcultures before subcutaneous implantation. However, two animals underwent ^{18}F-Fluorodeoxyglucose microPET and showed no significant radiotracer uptake in the xenograft (data not showed). Such finding is not typical for malignant tumors including malignant insulinomas. Discordant results between *in vivo* and *in vitro* experiments have also been reported in the evaluation of carbidopa effects on BON cells and the related xenograft tumor (*11*).

Collantes et al. (*15*) reported the result of ^{18}F-FDOPA PET in two nude mice with RIN-

m5F insulinoma xenograft. PET was positive in both mice showing ^{18}F-FDOPA uptake about 60 min post ^{18}F-FDOPA i.v. injection. Neither dynamic PET acquisition nor carbidopa premedication was performed for further comparison with our results. Moreover this group reported a differential expression of type 2 vesicular monoamine transporters in RIN cells between *in vitro* and *in vivo* experiments consequently translational deductions have to be conducted with caution.

The limited number of mice, which underwent ^{18}F-FDOPA PET may represent a limitation of our study. Moreover, no animal was examined twice according to an intra-individual analysis with and without carbidopa premedication. However, the highly demanding care of the tumoral xenograft model, which was characterized by elevated mortality due to severe hypoglycemia before the appearance of measurable insulinoma xenograft, justify our study protocol.

CONCLUSION

In conclusion, carbidopa does not influence the ^{18}F-FDOPA uptake accumulation in RIN-m5f cells *in vitro* but improves tumor imaging *in vivo*. Our findings increase the current knowledge about ^{18}F-FDOPA uptake profile of RIN-m5F cells and related xenograft model. The present work represents the first preclinical research specifically focused on the insulinoma with potential translational implication.

Acknowledgement

REFERENCES

1. Okabayashi T, Shima Y, Sumiyoshi T, et al. Diagnosis and management of insulinoma. *World J Gastroenterol*. 2013;19:829-837.

2. Kauhanen S, Seppänen M, Minn H, Nuutila P. Clinical PET imaging of insulinoma and beta-cell hyperplasia. *Curr Pharm Des*. 2010;16:1550-1560.

3. Christ E, Wild D, Reubi JC. Glucagon like peptide-1 receptor: an example of translational research in insulinomas: a review. *Endocrinol Metab Clin North Am*. 2010;39:791-800.

4. Koopmans KP, Neels ON, Kema IP, et al. Molecular imaging in neuroendocrine tumors: molecular uptake mechanisms and clinical results. *Crit Rev Oncol Hematol*. 2009;71:199-213.

5. Tessonnier L, Sebag F, Ghander C, et al. Limited value of 18F-F-DOPA PET to localize pancreatic insulin-secreting tumors in adults with hyperinsulinemic hypoglycemia. *J Clin Endocrinol Metab*. 2010;95:303-307.

6. Imperiale A, Sebag F, Vix M, et al. ^{18}F-FDOPA PET/CT imaging of insulinoma revisited. *Eur J Nucl Med Mol Imaging*. 2015;42:409-418.

7. Imperiale A, Bahougne T, Goichot B, Bachellier P, Taïeb D, Namer IJ. Dynamic 18F-FDOPA PET findings after carbidopa premedication in 2 adult patients with insulinoma-related hyperinsulinemic hypoglycemia. *Clin Nucl Med*. 2015;40:682-684.

8. Koopmans KP, Neels OC, Kema IP, et al. Improved staging of patients with carcinoid and islet cell tumors with 18F-dihydroxy-phenyl-alanine and 11C-5-hydroxy-tryptophan positron emission tomography. *J Clin Oncol*. 2008;26:1489-1495.

9. Kauhanen S, Seppänen M, Nuutila P. Premedication with carbidopa masks positive finding of insulinoma and beta-cell hyperplasia in [18F]-dihydroxy-phenyl-alanine positron emission tomography. *J Clin Oncol.* 2008;26:5307-5308.

10. Uccella S, Cerutti R, Vigetti D, et al. Histidine decarboxylase, DOPA decarboxylase, and vesicular monoamine transporter 2 expression in neuroendocrine tumors: immunohistochemical study and gene expression analysis. *J Histochem Cytochem.* 2006;54:863-875.

11. Neels OC, Koopmans KP, Jager PL, et al. Manipulation of [11C]-5-hydroxytryptophan and 6-[18F]fluoro-3,4-dihydroxy-L-phenylalanine accumulation in neuroendocrine tumor cells. *Cancer Res.* 2008;68:7183-7190.

12. Kuik WJ, Kema IP, Brouwers AH, et al. In vivo biodistribution of no-carrier-added 6-18F-fluoro-3,4-dihydroxy-L-phenylalanine (18F-DOPA), produced by a new nucleophilic substitution approach, compared with carrier-added 18F-DOPA, prepared by conventional electrophilic substitution. *J Nucl Med.* 2015;56:106-112.

13. de Vries EFJ, Luurtsema G, Brüssermann M, Elsinga PH, Vaalburg W. Fully automated synthesis module for the high yield one-pot preparation of 6-[^{18}F]-fluoro-l-DOPA. *Appl Radiat Isot.* 1999;51:389-394.

14. Gazdar AF, Chick WL, Oie HK, et al. Continuous, clonal, insulin- and somatostatin-secreting cell lines established from a transplantable rat islet cell tumor. *Proc Natl Acad Sci USA.* 1980;77:3519-3523.

15. Collantes M, Barajas M, Quincoces G, et al. Lessons from 11C-Dihydrotetrabenazine Imaging in a Xenograft Mouse Model of Rat Insulinoma: is PET Imaging of Pancreatic Beta Cell Mass Feasible? *Q J Nucl Med Mol Imaging.* 2015 Apr 17 (in press).

16. Fuchs BC, Bode BP. Amino acid transporters ASCT2 and LAT1 in cancer: partners in crime? *Semin Cancer Biol*. 2005;15:254-266.

17. Zheng G, Dwoskin LP, Crooks PA. Vesicular monoamine transporter 2: role as a novel target for drug development. *AAPS J*. 2006;10:E682-E692.

18. Nawashiro H, Otani N, Shinomiya N, et al. L-type amino acid transporter 1 as a potential molecular target in human astrocytic tumors. *Int J Cancer*. 2006;119:484-492.

19. Orlefors H, Sundin A, Lu L, et al. Carbidopa pretreatment improves image interpretation and visualisation of carcinoid tumours with 11C-5-hydroxytryptophan positron emission tomography. *Eur J Nucl Med Mol Imaging*. 2006;33:60-65.
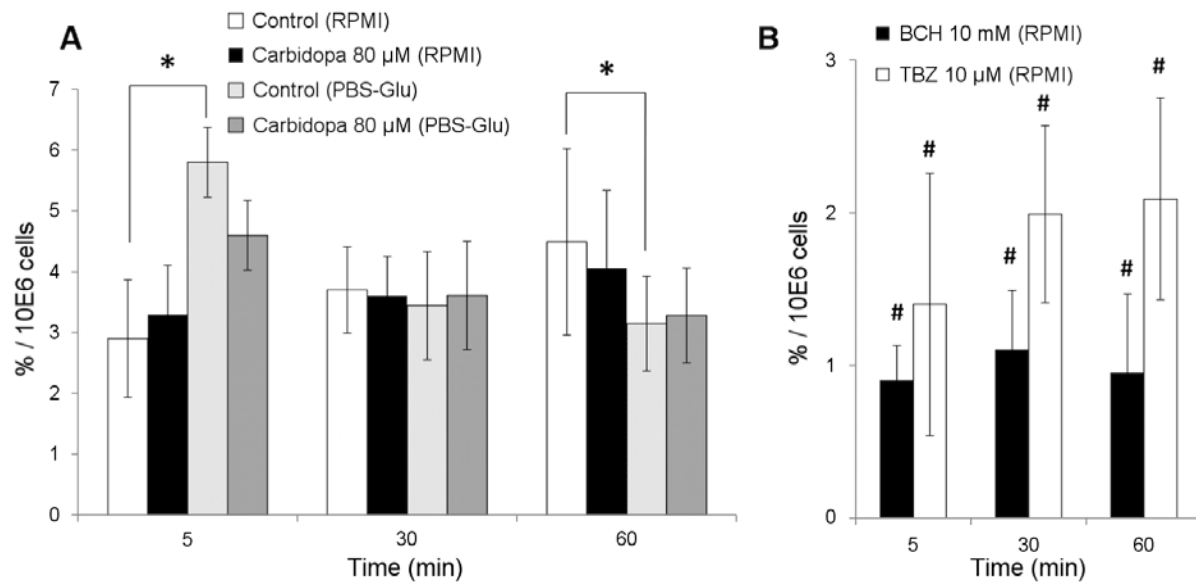
FIGURE 1. Accumulation of ^{18}F-FDOPA in RIN-5mF cells. Tracer accumulation was measured in classical Roswell Park Memorial Institute culture medium (RPMI) and amino acid free medium composed of phosphate buffer PBS and glucose (PBS-Glu). Values are expressed as mean percentage of uptake for 10^6 cells ± standard error of mean. **(A)** Effect of carbidopa (CD, 80 µM) on ^{18}F-FDOPA uptake in RPMI culture medium (n=12 for each condition) and in PBS-Glu medium (n=4 for each condition). *: $p<0.05$ (Mann-Whitney U test). **(B)** Effect of 2-aminobicyclo[2.2.1]heptane-2-carboxylic acid (BCH, 10 mM; n=4) and Tetrabenazine (TBZ, 10 µM; n=2) on ^{18}F-FDOPA uptake in RPMI culture medium. #: $p<0.05$ (Mann-Whitney U-test).
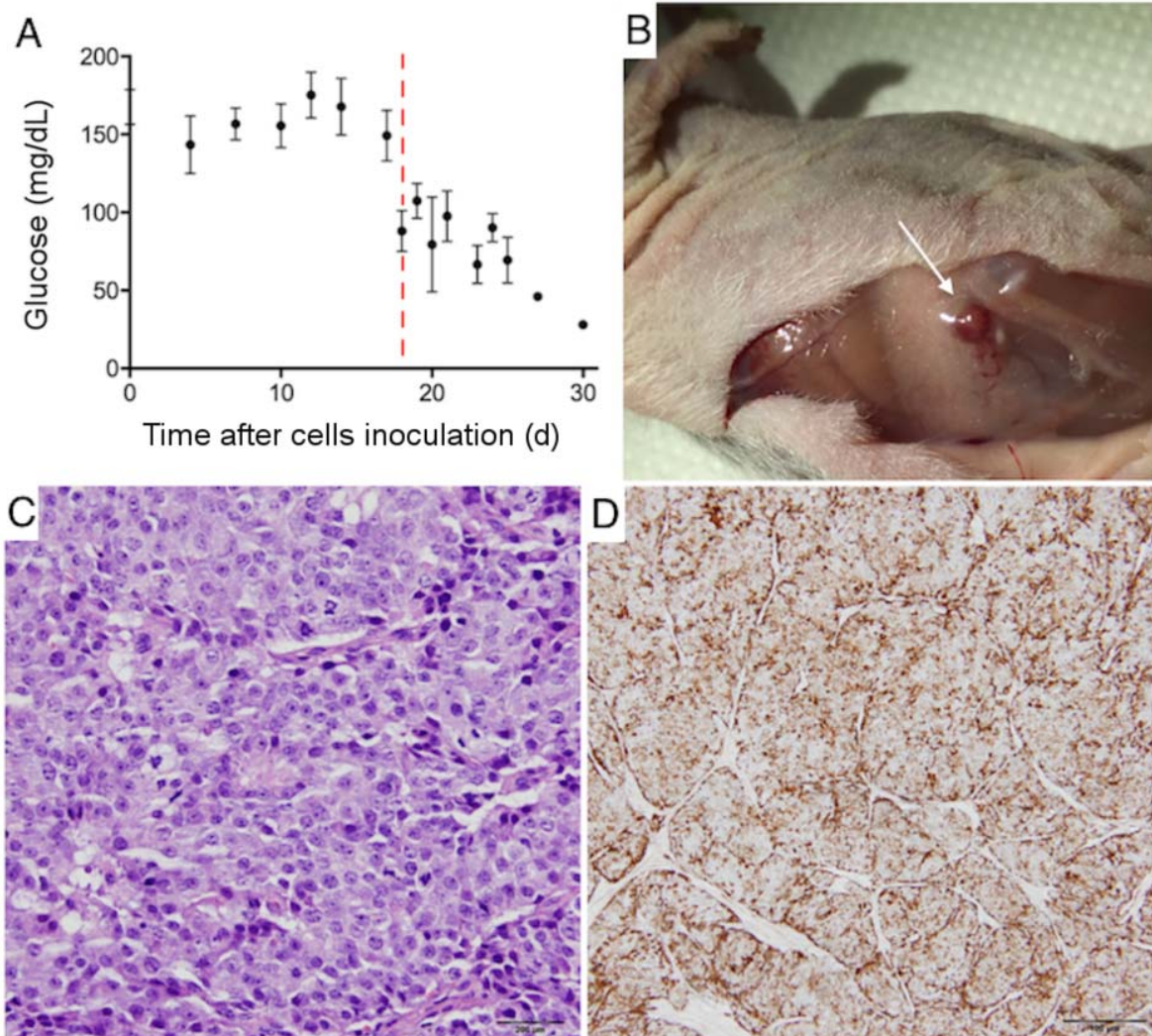
FIGURE 2. Functional and pathological characterization of insulinoma xenograft. **(A)** Morning serum glycemia levels from blood samples collected from ten non-fasted xenograft mice. The dotted line represents the introduction of 20% glucose solution instead of water. **(B)** Insulinoma xenograft of 1.4x1.3 mm (arrow) developed 15 days after the subcutaneous injection of 6 millions of RIN5-mF cells. Insulinoma-bearing mice deceased after hypoglycemic crisis (serum glycemia: 18 mg/dl). **(C)** Histological analysis of RIN5-mF xenograft tumor showing epithelioid and spindle cells (H&Ex400). **(D)** Immunohistochemical analysis of RIN5-mF xenograft tumor showing insulin positive immunostaining.
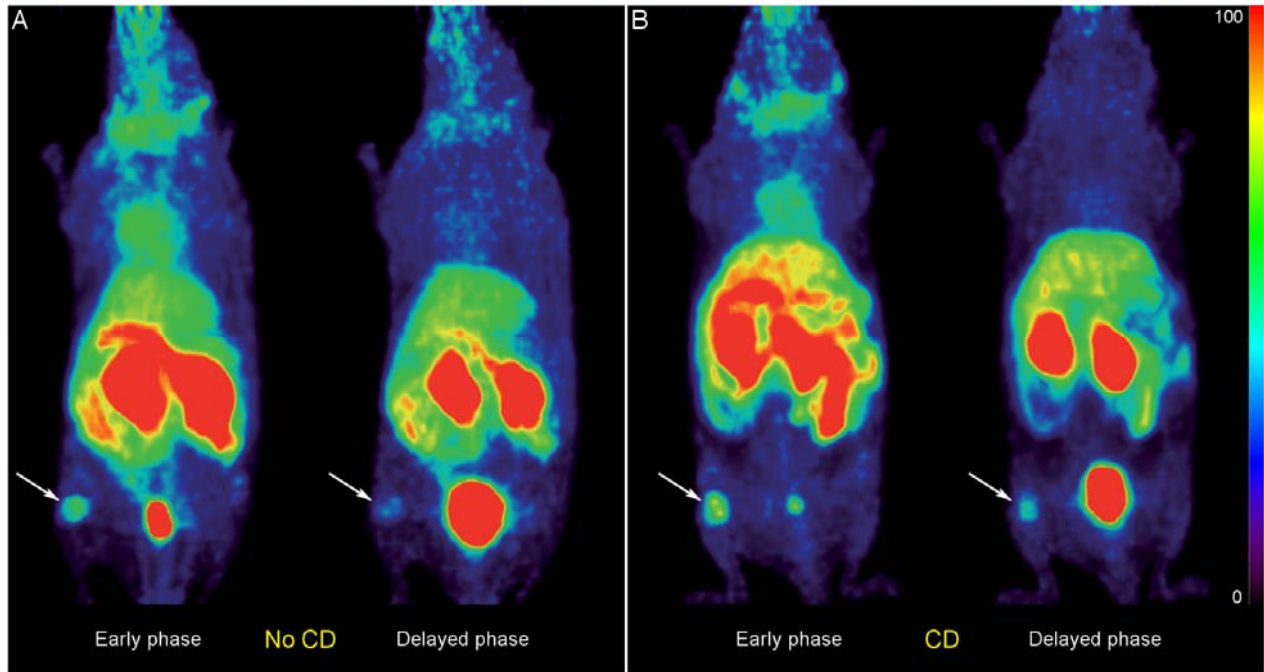
FIGURE 3. Representative anterior view of ^{18}F-FDOPA PET Maximum Intensity Projections images obtained without (**A**) and after carbidopa (CD) premedication (**B**) of two nude mice with subcutaneous insulinoma xenograft of 38 mm^3 and 52 mm^3, respectively, on the right hind leg (arrows). Images were reconstructed from summed time frames of 0-5 min (early-phase) and 15-20 min (delayed-phase) after ^{18}F-FDOPA i.v. injection. Insulinomas were detected irrespectively from carbidopa treatment. Moreover, tumor SUV from treated mice was higher than that from non-treated mice at both early and delayed PET acquisitions (SUV values: No-CD/early=0.94, No-CD/delayed=0.46, CD/early=1.46, CD/delayed=1.03).
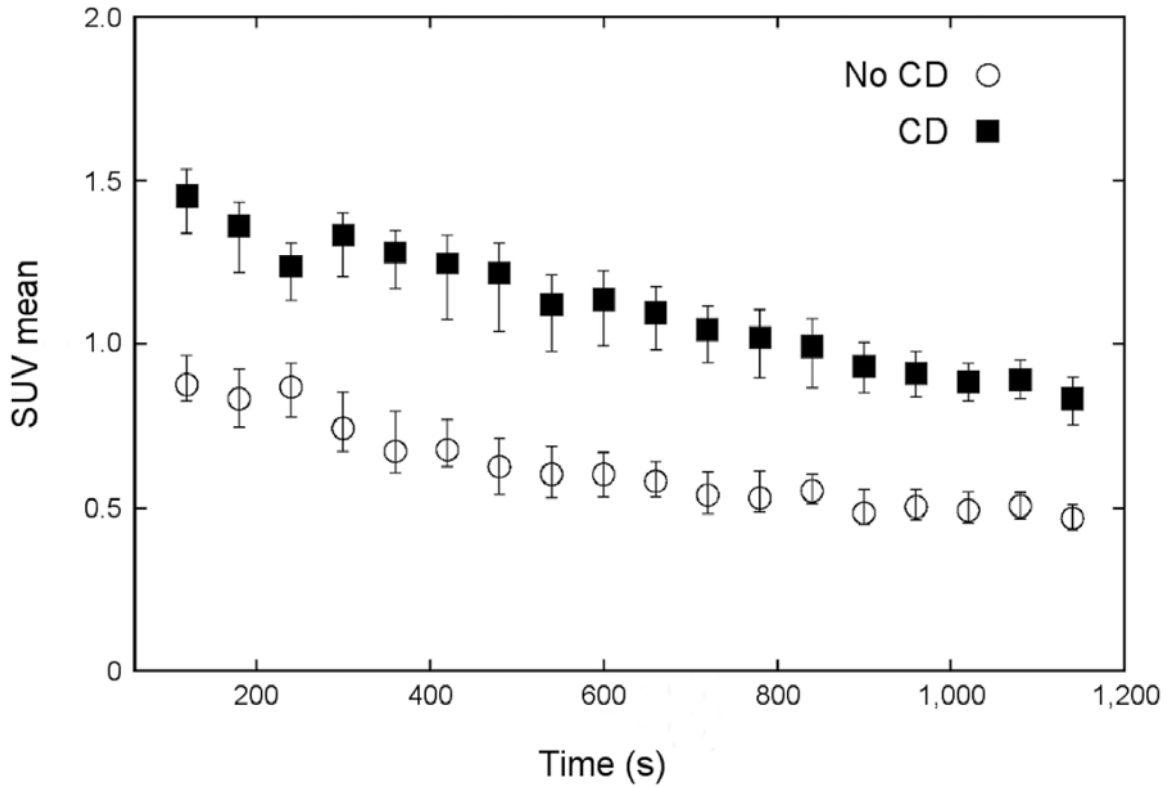
FIGURE 4. ^{18}F-FDOPA PET time activity curves of insulinoma xenograft according to carbidopa (CD) premedication (No CD vs. CD). Tumors from carbidopa-treated mice showed significantly higher ^{18}F-FDOPA uptake over the whole PET acquisition than tumors from non-treated mice ($p<0.05$). SUV values are indicated as median and interquartile range.
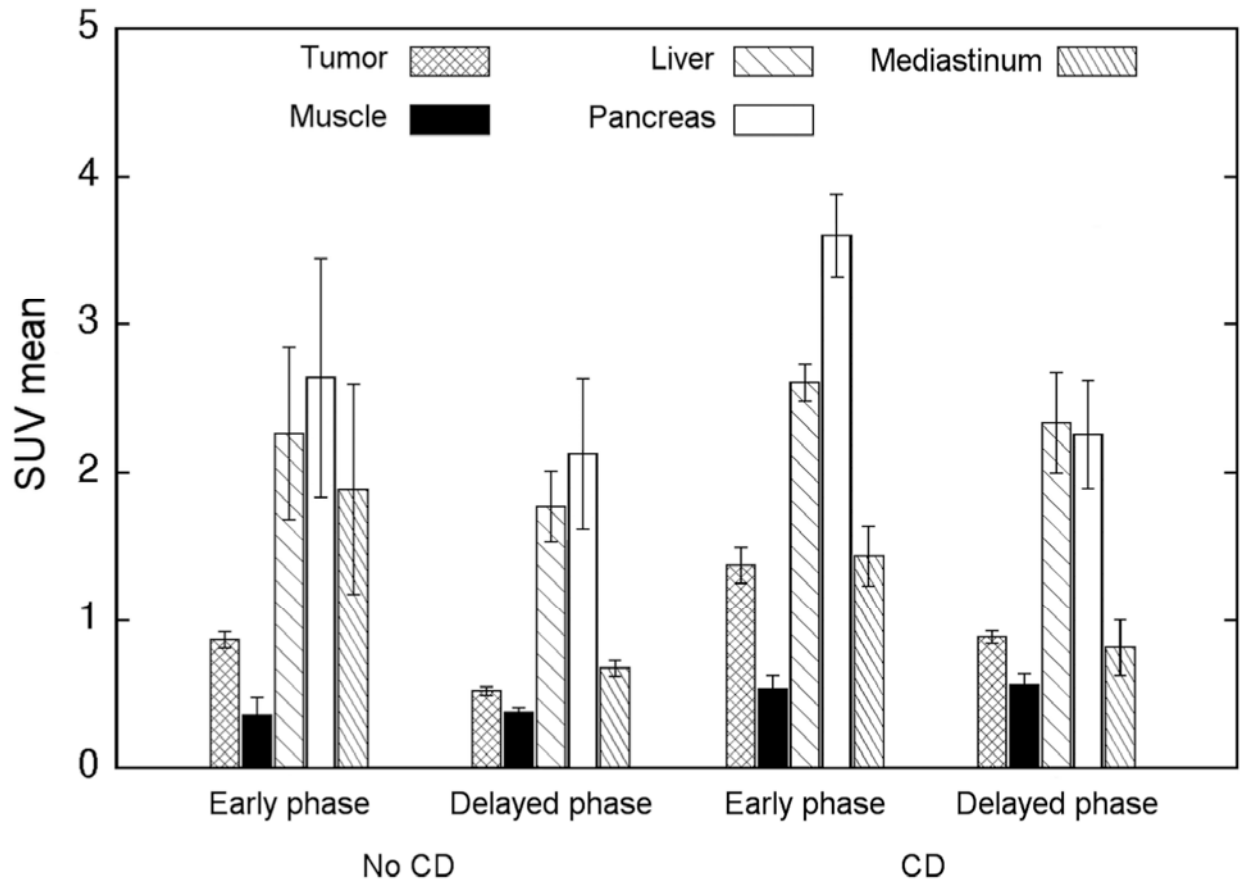
FIGURE 5. Biodistribution of ^{18}F-FDOPA in mice bearing insulinoma xenograft according to carbidopa (CD) premedication (No CD vs. CD). SUV values (mean ± standard error of mean) were obtained from summed time frames of 0-5 min (early-phase) and 15-20 min (delayed-phase) of the dynamic PET study after ^{18}F-FDOPA injection. ^{18}F-FDOPA degradation in peripheral organs is inhibited by carbidopa with consequent increase of radiotracer availability and accumulation in abdominal organs. Statistical significance was not reached probably because of the small number of analyzed animals.